

Yaw attitude modeling for BeiDou I06 and BeiDou-3 satellites

Chen Wang¹ · Jing Guo^{1,3}  · Qile Zhao^{1,2} · Jingnan Liu^{1,2}

Received: 28 November 2017 / Accepted: 5 September 2018
© Springer-Verlag GmbH Germany, part of Springer Nature 2018

Abstract

The estimated yaw angles of the BeiDou I06 satellite demonstrated that the satellite experienced midnight- or noon-turn maneuvers when the sun elevation angle above the orbital plane (β angle) was in the range of $[-3^\circ, +3^\circ]$ and the orbital angle was in the range of approximately $[-6^\circ, 6^\circ]$ or $[174^\circ, 186^\circ]$. The behavior of yaw attitude maneuvers in the vicinity of the midnight and noon points was identical. An alternative yaw attitude model similar to that used for the Galileo Full-Operation-Capacity (FOC) satellites was developed on the basis of the estimated BeiDou I06 yaw angles with an accuracy of approximately 3.4° to reproduce the yaw attitude behaviors. However, a discrepancy in the form of a reversal in yaw direction during the midnight-turn maneuver was observed for BeiDou I06 when the β angle was extremely small ($< 0.1^\circ$). The derived yaw attitude model was proved to model the yaw attitude of the BeiDou-3 experimental satellites, and reduces the observation residuals in the vicinity of the midnight and noon points to normal levels, and facilitates continuous satellite clock estimation during eclipse periods. Compared to the yaw attitude model developed by the European Space Operations Centre (ESOC), a similar performance has been achieved with maximum yaw differences up to 9.2° when the β angle is close to 0° . The average agreement between the models is about 1° . However, the ESOC model was developed based on a patented eclipsing model, the developed model in this study is open access.

Keywords Yaw attitude · BeiDou I06 · BeiDou-3 · Eclipse season

Introduction

Modeling a navigation satellite yaw attitude or orientation is essential for three reasons, first to correct the phase center variations, second to account for the phase wind-up effect (Wu et al. 1993), and third to model the non-gravitational perturbations that act on the spacecraft. In GNSS satellites, the Z-axis of the satellite body frame, with the same direction of the navigational antennas, points to the earth. The Y-axis is the rotational axis of the solar panels and normally is perpendicular to the sun–satellite direction. The X-axis completes the orthogonal right-handed system and points toward or against the sun hemisphere (Bar-Sever 1996;

Montenbruck et al. 2015). In combination, these requirements cause satellites to yaw constantly along the Z-axis. Usually, the onboard sun and earth sensors of the attitude control system are used to monitor the positions of the sun and earth, whereby the required orientation of the satellite can be determined. Using the momentum wheels, the satellite can be deployed to the required orientation. However, for GPS II/IIA satellites, once they are in the earth shadow, in which case the output of the sun sensors is essentially zero and the attitude control system is driven in an open loop mode by the noise in the system (Bar-Sever 1996), a specific shadow-crossing maneuver starts. In addition, for most GNSS satellites, once the required yaw rate exceeds the maximum hardware yaw rate and the attitude control system cannot deploy the satellite to the required orientation, additional maneuvers are required. As these usually occur in the vicinity of the midnight point (the farthest point from the sun in the satellite orbital plane) and noon point (the nearest point from the sun in the satellite orbital plane), these kinds of yaw maneuvers are termed as midnight- and noon-turn maneuvers.

✉ Jing Guo
jingguo@whu.edu.cn

¹ GNSS Research Center, Wuhan University, 129 Luoyu Road, Wuhan 430079, China

² Collaborative Innovation Center of Geospatial Technology, Wuhan University, 129 Luoyu Road, Wuhan 430079, China

³ School of Engineering, Newcastle University, Newcastle upon Tyne NE1 7RU, UK

Orbit-normal (ON) mode is used by the regional BeiDou, hereafter denoted as BeiDou-2, inclined geosynchronous orbit (IGSO) and medium earth orbit (MEO) satellites when the sun elevation angle with respect to the orbital plane (β angle) is in the range of $[-4^\circ, +4^\circ]$ (Guo et al. 2013). It is quite a simple yaw attitude control mode compared to the yaw models adopted by other GNSS satellites, i.e., shadow-crossing maneuver used by GPS BLOCK II/IIA (Bar-Sever 1996), midnight- and noon-turn maneuvers used by GPS BLOCK IIR (Kouba 2009), GPS BLOCK IIF (Dilssner et al. 2011a; Kuang et al. 2017), GLONASS-M (Dilssner et al. 2011b), and Galileo In-Orbit-Validation (IOV) and Full-Operation-Capacity (FOC) satellites (GSA 2017). In addition, the Japanese QZSS Michibiki satellite also uses the ON mode (Ishijima et al. 2009). In this case, the Z-axis of the body frame points to the radial direction and the X-axis points toward the along-track direction, which thus yields a zero yaw angle since the yaw angle is defined as the angle between the X-axis of the body frame and the instantaneous direction of the satellite's velocity vector. The Y-axis is perpendicular to the orbital plane and completes the right-handed frame. However, a dramatic degeneration in orbit accuracy can be observed when the attitude control mode is switched to ON mode for BeiDou IGSO and MEO satellites (Guo et al. 2013) as well as QZSS Michibiki satellite (Steigenberger et al. 2013) when the five-parameter ECOM solar radiation pressure (SRP) model is used. Although this issue can be overcome by properly modeling non-gravitational perturbations, in particular the SRP as previously done for the QZSS Michibiki satellite (Montenbruck et al. 2017b; Zhao et al. 2017) as well as for BeiDou-2 IGSO and MEO satellites (Guo et al. 2017), the orbit accuracy is still low for those POD arcs containing the attitude mode transition epoch. Hence, the ultimate solution is to use a continuous attitude control model. It is what new-generation BeiDou satellites (hereafter denoted as BeiDou-3) have done; this was confirmed by Zhao et al. (2018). Estimations of the yaw angles demonstrated that BeiDou-3 experimental satellites experienced identical midnight- and noon-turn maneuvers when the β angle was approximately between -3° and $+3^\circ$. Unfortunately, owing to limitations of the available tracking stations, the accuracy of the estimated yaw angle was approximately 10° , which made it hard to develop a precise yaw attitude model for BeiDou-3 satellites.

Recently, a significant degeneration in the orbit accuracy of the BeiDou I06 satellite (PRN C13, formerly C15) submitted by Wuhan University to the International GNSS Service (IGS) Multi-GNSS Experiment (MGEX, Montenbruck et al. 2017a) was observed at the end of June 2017, when the β angle was between -4° and $+4^\circ$. Moreover, the quality of I06 orbits from the Center for Orbit Determination in Europe (CODE) and GeoForschungsZentrum Potsdam (GFZ) also exhibited a similar degeneration. It can be confirmed that

the ON mode was used by Wuhan University to generate the I06 orbit and clock products in this period. As an additional constrained constant acceleration in the along-track direction has been introduced into the five-parameter Extended CODE Orbit Model (ECOM) SRP model to improve the orbit quality of BeiDou-2 IGSO and MEO satellites in ON mode by Wuhan University (Guo et al. 2016), the orbit degeneration of BeiDou I06 indicates that a different attitude model may be used by I06 instead of ON mode in this period. This has been confirmed by Liu et al. (2017), but they did not present the yaw attitude control model. This inspired us to investigate the yaw attitude behavior of the satellite. In addition, we suspect that the same yaw attitude control model was used by the BeiDou-3 experimental IGSO and MEO satellites, as I06 was launched on March 29, 2016, when four BeiDou-3 experimental satellites had already been successfully deployed. When this study was under review, the European Space Operations Centre (ESOC) published a yaw model for BeiDou I06 (hereafter denoted as ESOC model) (Dilssner 2017), and further validated its applicability for BeiDou-3 experimental satellites (Dilssner et al. 2018). The model, as pointed by Kouba (2017), is based on the patented eclipsing model (Ebert and Oesterlin 2005). Hence, it might be problematic to use it in a public scientific or commercial software, such as the widely used ECLIPS subroutine within GNSS community (Kouba 2017).

Hence, the aim of this study is to establish a yaw attitude model to reproduce the yaw attitude behavior of I06 on the basis of an analysis of the estimated yaw angles, and can be freely used without copyright issue. The applicability to BeiDou-3 experimental satellites to the developed yaw attitude model will be validated by comparison with the yaw angles estimated by Zhao et al. (2018). Furthermore, the developed model will be compared with the ESOC model.

Nominal yaw attitude

The nominal yaw angle Ψ_n is defined as the angle between the X-axis of the satellite body frame and the instantaneous direction of the satellite's velocity vector. Following the IGS convention for the orientation of a GNSS satellite body frame in space (Montenbruck et al. 2015), the nominal yaw angle and yaw rate $\dot{\Psi}_n$ are given by the following expressions (Bar-Sever 1996):

$$\begin{aligned}\Psi_n &= \text{ATAN2}(-\tan \beta, \sin \mu) \\ \dot{\Psi}_n &= \frac{\dot{\mu} \tan \beta \cos \mu}{\sin^2 \mu + \tan^2 \beta}\end{aligned}\quad (1)$$

for a given β angle, where the orbital angle μ is the argument of the latitude of the satellite with respect to the midnight

point in the orbital plane, and the average orbital angular velocity $\dot{\mu}$ is obtained as follows:

$$\begin{aligned}\dot{\mu} &= \sqrt{\frac{GM}{a^3}} \\ a &= \frac{r}{2 - \frac{rv^2}{GM}}\end{aligned}\quad (2)$$

where r and v are the scalar quantities for geocentric position and velocity of the satellite and GM is the gravitational constant of the earth. $\text{ATAN2}(b, c)$ is the FORTRAN function for $\arctan(b, c)$, which gives a signed angle in the range $[-180^\circ, +180^\circ]$. The value of Ψ_n reaches local maxima when the satellite is at the noon point and midnight point. Once the nominal yaw attitude rate exceeds the maximum yaw rate of the momentum wheels, yaw maneuvers take place, which usually occur in the vicinity of the noon and midnight points. Except for GPS Block II/IIA, most GPS, GLONASS, and Galileo satellites only experience these two kinds of yaw attitude maneuvers when the satellites are in eclipse periods. A satellite starts to enter an earth eclipse season when the β angle approximately meets the following condition (Kouba 2009):

$$|\beta| \leq \frac{R_E}{r} \quad (3)$$

where R_E is the average radius of the earth. Hence, the I06 satellite will go through the earth's shadow when the β angle is in the approximate region of $(-8.5^\circ, +8.5^\circ)$, as shown in Fig. 1.

Data processing

For the estimation of yaw angles, the reverse kinematic precise point positioning (RKPPP) approach (Dilssner et al. 2011b) was used in this study. Precise orbit determination (POD) is a prerequisite step for this approach. Once the orbit is precisely determined, RKPPP will be performed to

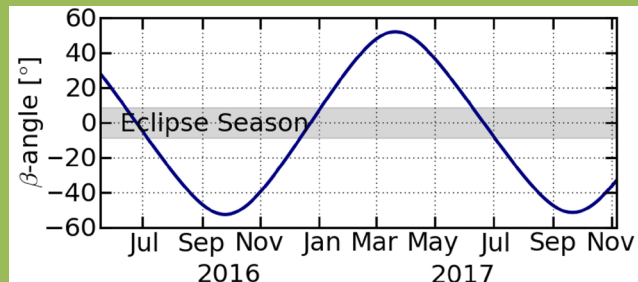


Fig. 1 Evolution of the sun elevation angle (β angle) with respect to the I06 orbital plane from June 2016 until November 2017

estimate the epoch-wise phase center offset (PCO) as well as the satellite clock offset with other parameters, e.g., orbit parameters, earth orientation parameters, station coordinates, receiver clocks, troposphere parameters, and ambiguities fixed at the values estimated in the POD step. The POD strategy used has already been clearly documented by Guo et al. (2016). The differences to be addressed here included the sampling interval and PCO, as well as the tracking stations used. Observations with a sampling rate of 30 s were used to study the actual yaw attitude behavior of the I06 satellite. A calibrated PCO of (586.4, 0.0, 2896.2) mm was used for this satellite. As the ground track of I06 mainly lies in the Asia-Pacific region, the BeiDou Experimental Tracking Network (BETS) and Crustal Movement Observation Network of China (CMONOC) were used. To improve the coverage further, the IGS MGEX network (Montenbruck et al. 2017a) was also employed. Figure 2 shows the distribution of 65 stations tracking I06. Until November 2017, the I06 satellite has experienced three eclipse seasons, which extended from day of year (DOY) 165 to 187, 2016, DOY 347, 2016 to 002, 2017, and DOY 160 to 182, 2017. Hence, only data from these periods were processed to investigate the yaw attitude behavior. The differences between the estimated and nominal yaw angles excluding that in the vicinity of the midnight and noon points indicate that the accuracy of the estimated yaw angles is better than 3° (root mean square, RMS).

Yaw maneuvers

In this section, the behavior of the estimated yaw angles in the vicinity of the midnight and noon points is analyzed to get an insight into the laws governing the yaw attitude of the satellite.

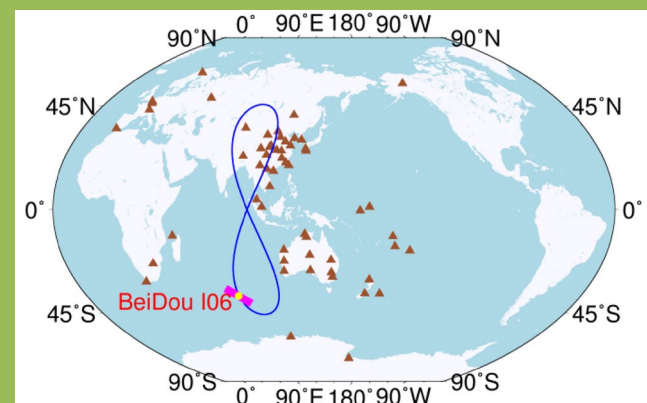


Fig. 2 Distribution of stations tracking the BeiDou I06 satellite, as well as the ground track of I06

Midnight-turn maneuvers

The evolution of the estimated and nominal yaw angles of the I06 satellite during its passage through the earth's shadow is depicted in Fig. 3. Before entry into the earth's shadow, the estimated and nominal yaw angles are nearly identical, and the satellite is essentially able to maintain its nominal yaw attitude while passing through the earth's shadow until the β angle is in the range $[-3^\circ, +3^\circ]$, then a clear departure from the nominal attitude is observed. It seems that the satellite starts and finishes maneuver at fixed orbital angles (approximately -5° and 5°) to keep the actual yaw angle at the orbit's midnight point equal to $\pm 90^\circ$. This ensures that the maximum deviation between the actual and nominal yaw angles throughout the maneuver is as small as possible and thus reduces the impact on the users, but results in a variable yaw rate. The direction of the actual yaw maneuver is the same as that of the nominal yaw attitude. At $\beta \approx 0^\circ$, the midnight-turn maneuver lasts for approximately 40 min. For $\beta \neq 0^\circ$, the time required for the yaw maneuver is shorter.

The yaw attitude behavior of I06 was found to be almost identical during the three eclipse seasons. However, a discrepancy, shown in Fig. 4, was observed for the midnight-turn maneuver on DOY 171, 2017, when the β angle was less than 0.1° . The observed midnight-turn maneuver displayed the opposite yaw direction from the nominal direction. This is the only one midnight-turn maneuver that was observed to exhibit a wrong turn direction. A poor accuracy orbit used as the input of the attitude control system might account for this issue, but it still needs to be investigated further.

Fig. 3 Estimated (blue dot) and nominal (red line) yaw angles of I06 crossing the earth's shadow at different β angles

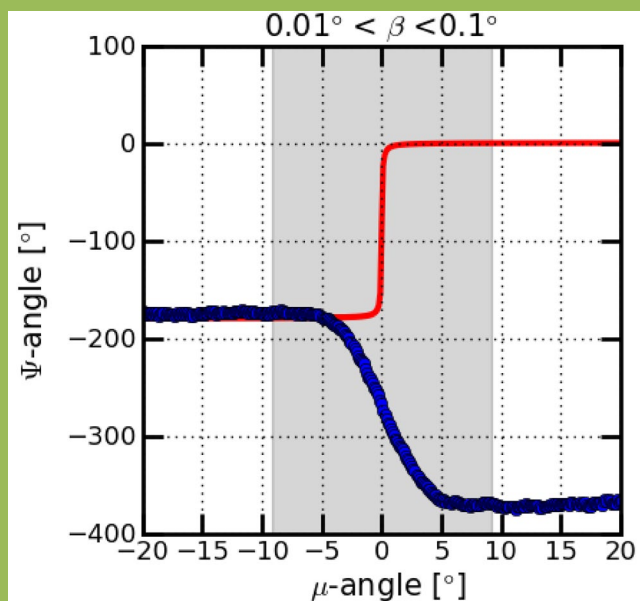
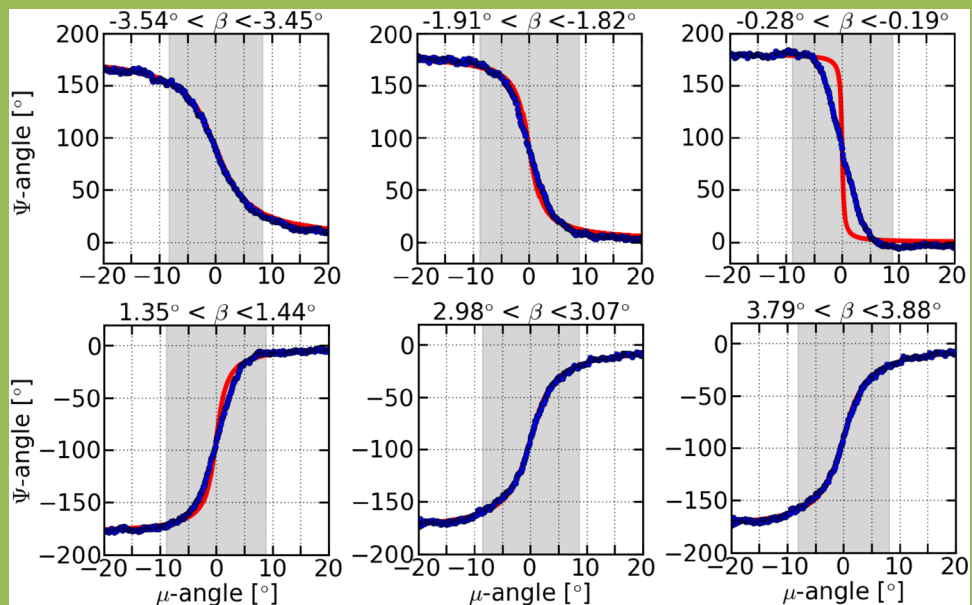
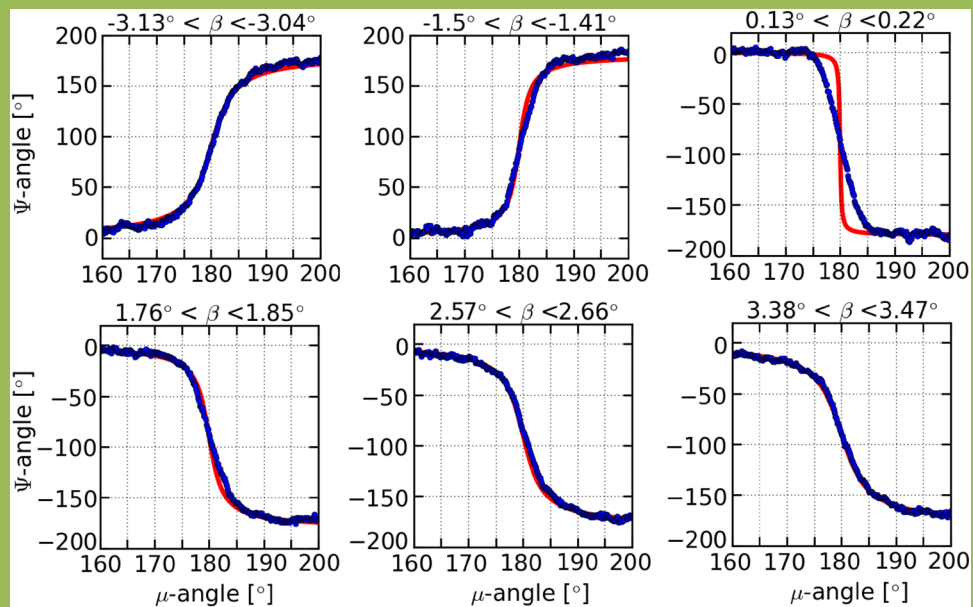


Fig. 4 Observed discrepancy in the form of a reversal in the direction of the midnight-turn yaw maneuver of I06 on DOY 171, 2017. The red line shows the nominal yaw angles. The blue dots show the estimated yaw angles

Noon-turn maneuvers

The evolution of the estimated and nominal yaw angles of the I06 satellite during its passage around the noon point at various small β angles from -3.13° to 3.47° is illustrated in Fig. 5. In general, almost the same behavior was observed for noon-turn maneuvers as for midnight-turn maneuvers. The satellite starts and ends noon-turn maneuvers with a direction identical to the nominal direction when the β angle

Fig. 5 Estimated (blue dot) and nominal (red line) yaw angles of I06 crossing the noon point at different β angles



lies in the range of $[-3^\circ, +3^\circ]$, and the orbital angle reaches the threshold values of approximately 175° and 185° . The actual yaw angle at the noon point in the orbit equals the nominal value ($\pm 90^\circ$). This helps to reduce the impact of yaw maneuvers on the users.

In contrast to the midnight-turn maneuvers, all the observed noon-turn maneuvers displayed the same yaw direction as the nominal direction, and no discrepancy in the form of a wrong yaw direction was observed. However, it is necessary to note that all the noon-turn maneuvers occurred when the β angle was greater than 0.1° during our investigation.

Yaw attitude model

In October 2017, the European Global Navigation Satellite Systems Agency released metadata for the Galileo IOV and FOC satellites, which included a yaw attitude control model for Galileo FOC satellites equivalently expressed as follows:

$$\begin{aligned} \psi(\mu) = & 90^\circ \cdot \text{SIGN}(1, \psi(\mu_s)) \\ & + [\psi(\mu_s) - 90^\circ \cdot \text{SIGN}(1, \psi(\mu_s))] \\ & \cdot \cos\left(\frac{2\pi}{t_{\max}} \cdot \frac{\mu - \mu_s}{\dot{\mu}}\right) \end{aligned} \quad (4)$$

where μ_s is the orbital angle at the start of the yaw maneuver, $\Psi(\mu_s)$ is the associated nominal yaw angle, $\text{SIGN}(a, b)$ is the usual FORTRAN function returning the value of a with the sign of b , and t_{\max} is a constant that represents the maximum yaw maneuver time which is 5656 s for Galileo FOC satellites. Once the β angle lies in the region of $(-4.1^\circ, 4.1^\circ)$ and the orbital angle lies in the range of $(-10^\circ, 10^\circ)$ or $(170^\circ,$

$190^\circ)$, the midnight- and noon-turn yaw maneuvers start for Galileo FOC satellites (GSA 2017). Figure 6 illustrates the nominal and modeled yaw angles in the vicinity of the midnight and noon points for Galileo E22 on DOY 172, 2017. By comparing with the estimated yaw angles illustrated in Figs. 3 and 5 for BeiDou I06 satellite, similar yaw behaviors can be observed. The satellite starts and ends yaw maneuvers with a direction identical to the nominal direction, and the actual yaw angle at the midnight or noon points in the orbit equals the nominal value ($\pm 90^\circ$). Hence, it can be concluded that BeiDou I06 and Galileo FOC satellites obey similar yaw attitude laws.

In (4), μ_s dominates the behavior of the yaw model, since t_{\max} is approximately equal to $|2m_s|/\dot{\mu}$ for the midnight-turn maneuver and $|2(\mu_s - 180^\circ)|/\dot{\mu}$ for the noon-turn maneuver when the β angle is nearly equals 0° . Hence, for modeling the yaw attitude of I06, it is essential to identify the value of μ_s . As illustrated in Figs. 3 and 5, satellite I06 starts its midnight- and noon-turn maneuvers at orbital angles of -5° and 175° , respectively. Hence, a series of yaw attitude models were established by decreasing μ_s from -5° or 175° in steps of 0.2° , and the differences between the modeled and estimated yaw angles were calculated. Finally, the best estimated model μ_s reaches 6° or 174° and the corresponding t_{\max} approximately equals 5740 s. Figure 7 shows the estimated yaw angles after removal of the nominal (red) and the modeled (blue) yaw values under a variety of β angles in $[-5^\circ, +5^\circ]$. The differences between the nominal and estimated yaw angles under low β angle would be in error by up to 90° . By contrast, the proposed model has the ability to predict the yaw angle with the same accuracy (about 3.4° in RMS) under a low β angle as it does under a higher β angle.

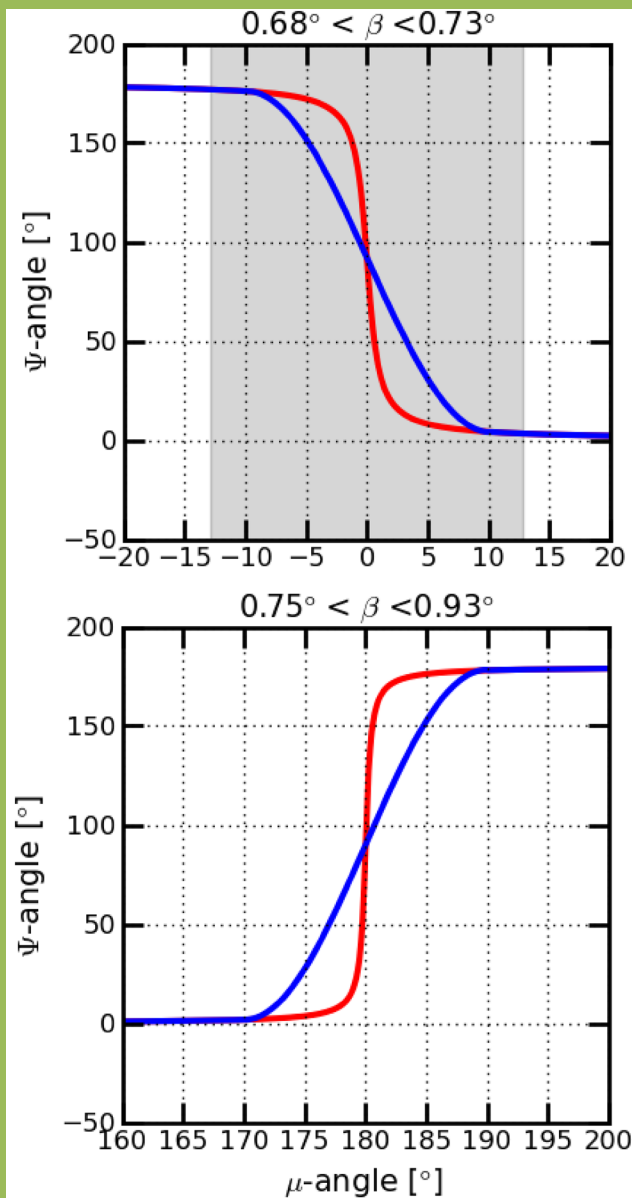


Fig. 6 Nominal (red line) and modeled (blue line) yaw angles for Galileo E22 satellite on DOY 172, 2017 in the vicinity of midnight (top) and noon points (bottom)

Please kindly note that the discrepancy illustrated in Fig. 4 is omitted in the plot.

Furthermore, the applicability to the BeiDou-3 experimental satellites of the model has been validated by comparing the modeled and estimated yaw angles. As illustrated in Fig. 8 for BeiDou I2-S (C32, top) and BeiDou M2-S (C33, bottom), the model reproduces the yaw attitude behaviors of the BeiDou-3 experimental satellites quite well. Statistically, by removing yaw attitudes estimated by fewer than eight tracking stations, the RMS of the differences between the modeled and estimated yaw attitudes is approximately 5°. This indicates that the model can also reproduce the

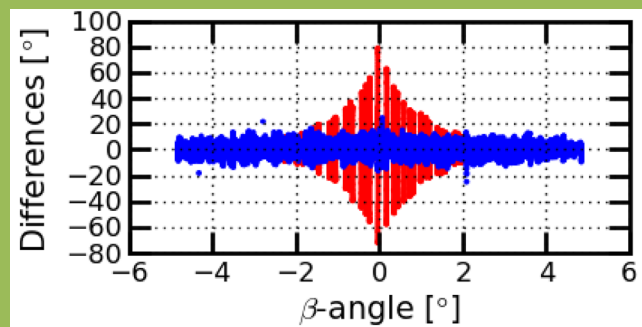


Fig. 7 Estimated yaw angles with respect to the nominal (red dot) and estimated (blue dot) yaw angles for BeiDou I06 satellite under a variety of β angles

yaw behaviors of the BeiDou-3 experimental satellites. It should be noted that, in contrast to BeiDou I06 and I2-S, the BeiDou M2-S is a MEO satellite, and the corresponding t_{\max} value is approximately 3090 s. Hereafter, the developed model is named WHU model, and will be compared with the ESOC model in the next section.

Comparison with ESOC model

As mentioned in “Introduction”, an alternative continuous yaw steering model for BeiDou I06 has been proposed by Dilssner (2017). In this model, to keep the change rate of the yaw angle at noon and midnight points from becoming infinitely large, a ‘smooth factor’ f has been introduced to calculate a modified β angle, β_d , to replace the actual one in (1) for yaw angle computation as follows:

$$\beta_d = \beta + f \cdot (\text{SIGN}(\beta_0, \beta) - \beta) \quad (5)$$

where β_0 is the critical sun elevation angle for yaw maneuvers. This model guarantees seamless transition from nominal yaw steering to smoothed yaw steering and vice versa. The key parameters that govern the model are β_0 and f . Slightly different from the expression in Ebert and Oesterlin (2005), the smooth function for BeiDou I06 is as follows:

$$f = \begin{cases} \frac{1}{1+d \cdot \sin^4 \eta} & \text{for } \beta_0 \leq |\beta| \\ 0 & \text{for } \beta_0 \leq |\beta| \end{cases} \quad (6)$$

where $d=80,000$ is a dimensionless constant, and β_0 equals 2.8°. Recently, it has been confirmed that the model can be used to predict the yaw attitudes of the BeiDou-3 I2-S satellite during midnight and noon-point yaw maneuvers (Dilssner et al. 2018). Figure 9 shows the ESOC model values after removal of the estimated (blue) and WHU model (red) values under a variety of β angles in $[-5^\circ, +5^\circ]$. With respect to the estimated yaw angles, similar performance has been observed for ESOC model and WHU model. The ESOC

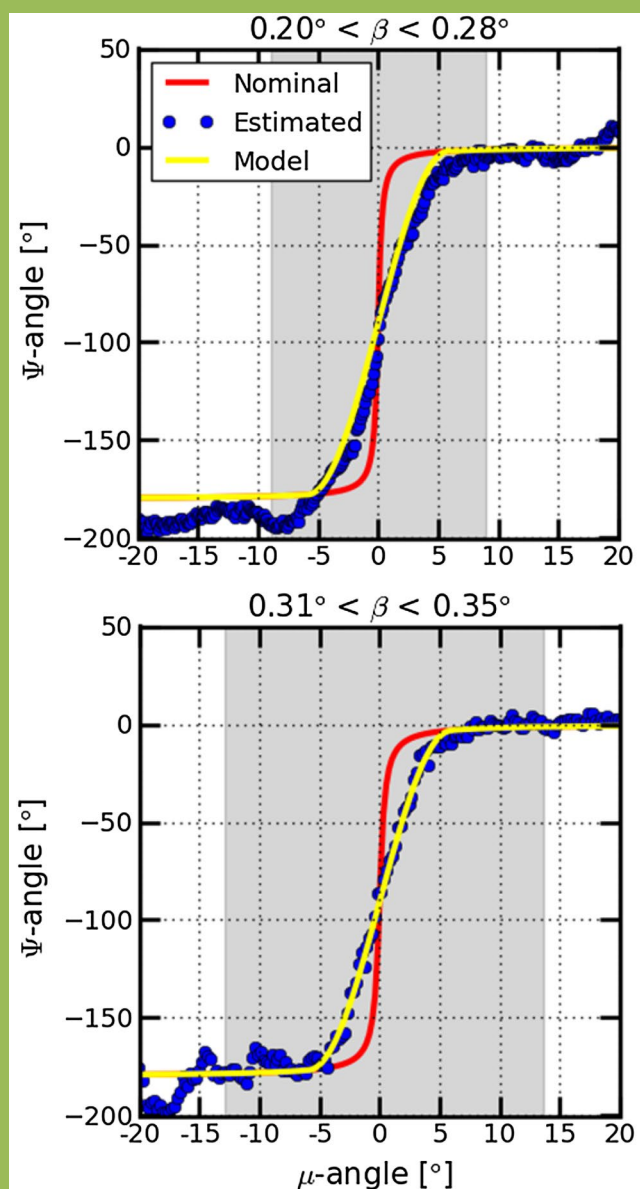


Fig. 8 Nominal (red line), estimated (blue dot), and modeled (yellow line) yaw attitudes of (top) BeiDou I2-S (C32) on DOY152, 2017 and (bottom) BeiDou M2-S (C33) satellites on DOY 180, 2017

model also has the ability to predict the yaw angle with the same accuracy under a variety of β angles. The accuracy in RMS is about 3.5° , and almost the same accuracy has been reached by the WHU model. With respect to the WHU model, the maximum difference can reach about 10° under low β angle, and the agreement in RMS is about 1° . This indicates that similar performance has been achieved by ESOC and WHU models.

Compared with ESOC model, WHU model uses different t_{\max} for IGSO and MEO satellites, while the same values of parameters are used in the ESOC model for both MEO and

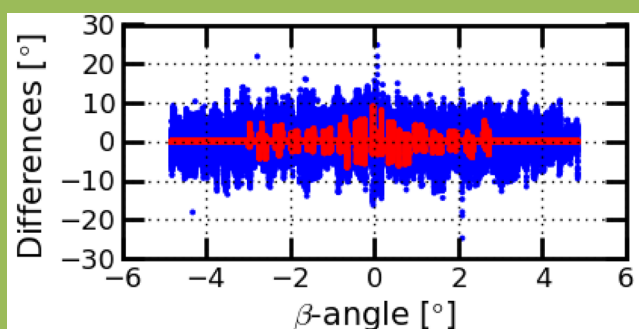


Fig. 9 ESOC yaw angles with respect to the WHU model (red dot) and estimated (blue dot) yaw angles for BeiDou I06 satellite under a variety of β angles

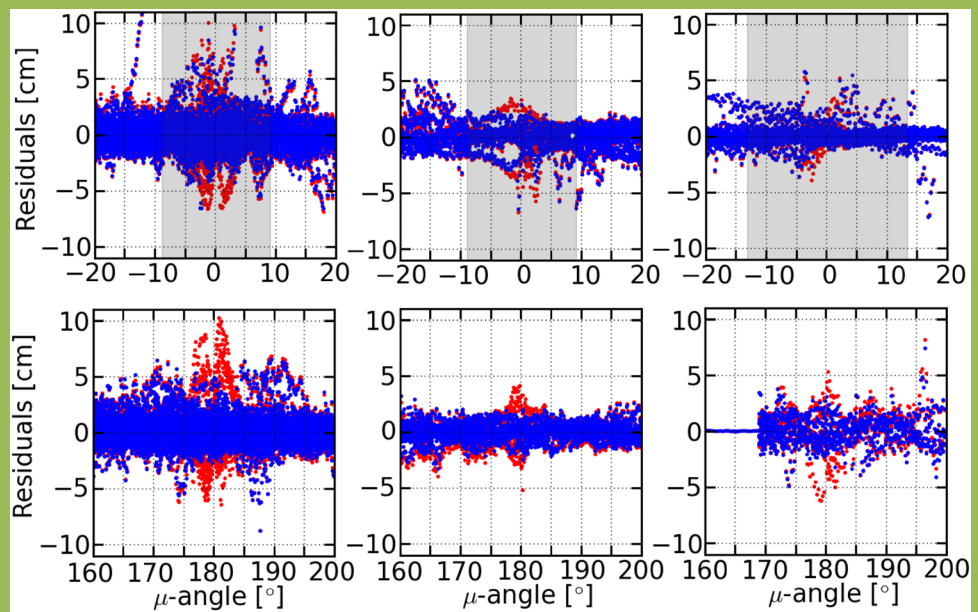
IGSO satellites. That is a minor disadvantage over the ESOC model which uses same model equation valid for both IGSO and MEO satellites. However, as stated by Kouba (2017), it might be problematic using the ESOC model in a public scientific or commercial software since it is developed based on the patented model. The WHU model has no such limitation, as it is developed based on the public released Galileo FOC model. In addition, since WHU model has the same functional equation as the yaw model of Galileo FOC satellites, it will facilitate the software implementation, as same software codes can be used for Galileo FOC and BeiDou-3 IGSO/MEO satellites.

Validation

For validation purposes, two kinds of orbit and clock solution were assessed with or without the yaw maneuver model using data during the eclipse periods for both BeiDou I06 and the BeiDou-3 experimental satellites. As previously mentioned, almost the same performance has been achieved by both the WHU and ESOC models for modeling yaw maneuvers. Hence, only the WHU model has been validated for BeiDou I06 and BeiDou-3 experimental satellites.

The errors that arise from mismodeling of the satellite antenna phase center owing to an erroneous yaw angle should propagate into the carrier phase residuals. When the nominal yaw attitude model is employed, a considerable increase in ionospheric-free phase residuals in the vicinity of the midnight and noon points can be observed, as shown in Fig. 10 for the I06 (left), I2-S (middle), and MS-2 (right) satellites near midnight (top) and noon (bottom) points. Here, it can be seen that when the nominal yaw attitude was used during the eclipse period, the maximum errors were almost 10 cm for I06 but less than 5 cm for the other two satellites. This was caused by different magnitudes of the PCO component on the X-axis of the satellite body frame, whereas the PCO components on the Y-axis were almost

Fig. 10 Ionospheric-free phase residuals with (red) nominal orientation and (blue) the proposed yaw maneuver model for the (top) midnight-turn and (bottom) noon-turn maneuvers of the (left) I06, (middle) I2-S, and (right) M2-S satellites

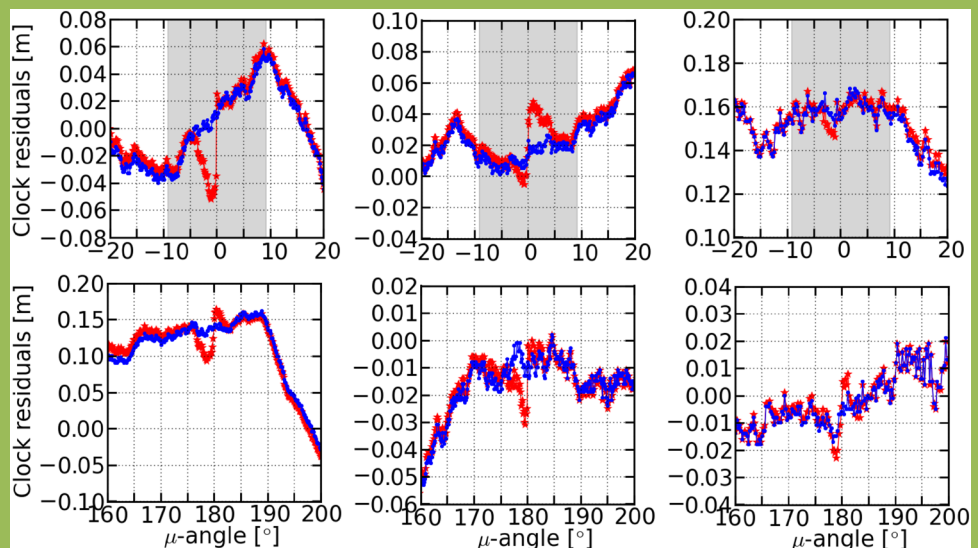


zero. For I06, the X-axis PCO component is approximately 57 cm, whereas it is approximately 30 cm and 20 cm for I2-S and M2-S, respectively (Zhao et al. 2018). In addition, it can be seen that the phase residuals are symmetrically distributed with respect to the midnight and noon points with local maxima at orbital angles of approximately $-1.5^\circ/1.5^\circ$ and $178.5^\circ/181.5^\circ$, which matches the characteristics of the yaw attitude behaviors quite well as shown in Figs. 3 and 5. With the new yaw attitude model, the errors were considerably smaller, and the magnitudes of the phase residuals inside and outside the yaw maneuver period were consistently comparable.

On the other hand, the satellite clock offsets are also impacted by errors from mismodeling of the phase wind-up effect and PCO due to an erroneous yaw angle

(Bar-Sever 1996; Kouba 2009). Figure 11 illustrates the clock residuals after the removal of the linear trend for the I06 (left), I2-S (middle), and M2-S (right) satellites near midnight (top) and noon (bottom) points. It can be clearly seen that there are large clock resets (jumps) in the vicinity of the midnight and noon points. In a similar way to the phase residuals, the magnitudes of clock resets are also related to the PCO values. The overall effect caused by both phenomena on clock estimation is less than 1 dm as seen in Fig. 11. However, the solutions using the yaw attitude model did not experience any problems and varied continuously and smoothly. These results confirm that the established yaw model can reproduce the actual yaw behavior of the I06 and BeiDou-3 experimental satellites quite well.

Fig. 11 Detrended clock residuals with (red) nominal orientation and (blue) the proposed yaw maneuver model for the (top) midnight-turn and (bottom) noon-turn maneuvers of the (left) I06, (middle) I2-S, and (right) M2-S satellites



Conclusion and discussion

Using the RKPPP approach, the yaw angles of the BeiDou I06 satellite were estimated. On the basis of the estimated yaw angles, a yaw attitude model that has a similar formulation to that used for the Galileo FOC satellites has been developed. In general, the established model can reproduce the actual yaw behaviors of I06 with an accuracy of around 3.4° . However, a discrepancy in the form of a reversal in the yaw direction of the midnight-turn maneuver was observed for I06 when the β angle was extremely small ($< 0.1^\circ$). As only one such event was observed, we have not modeled this discrepancy and have left it for further investigation. More important, the derived yaw attitude model was proved to be appropriate to model the yaw attitude of the next-generation BeiDou-3 satellites. By implementing the model in our PANDA software (Liu and Ge 2013), the observation residuals in the vicinity of the midnight and noon points were reduced to normal levels, and satellite clock estimation during eclipse periods became smoother.

Compared with the ESOC model, similar performance has been achieved by the developed WHU model. On the one hand, WHU model is developed on the basis of Galileo FOC yaw steering law and it will facilitate the software implementation, as the same software codes can be used for both satellites with specific threshold used for BeiDou IGSO or MEO satellites. The ESOC model, on the other hand, does have an advantage over the WHU model in that it uses the same model value for both BeiDou IGSO and MEO ones. However, the ESOC model is based on the patented eclipsing model which might make it problematic to use it in a public scientific or commercial software, whereas the developed WHU model can be used freely, such as the widely used ECLIPS subroutine in the GNSS community (Kouba 2017).

Recently, Dilssner (2017) noticed that a few BeiDou-2 satellites abandoned the ON model for using the continuous yaw steering model. Further monitoring of the yaw attitude of these second-generation satellites will be necessary in the future. In addition, it should be noted that BeiDou-3 satellites are based on two different satellite buses developed by the China Academy of Space Technology (CAST) and the China Academy of Science (CAS), whereas BeiDou M2-S and I2-S satellites are all based on the CAST platform as already analyzed in this study. The applicability of the developed yaw model to the BeiDou-3 satellites using the CAS platform still needs further validation.

Acknowledgements The IGS MGEX, iGMAS, and CMONOC are greatly acknowledged for providing the multi-GNSS data. The research is partially supported by the National Natural Science Foundation of China (Grant nos. 41504009 and 41574030). The numerical calculations in this paper have been done on the supercomputing system in the Supercomputing Center of Wuhan University. Finally, the authors

are also grateful for the comments and remarks of two reviewers and editor, which helped to significantly improve the manuscript.

References

- Bar-Sever YE (1996) A new model for GPS yaw attitude. *J Geodesy* 70(11):714–723. <https://doi.org/10.1007/BF00867149>
- Dilssner F (2017) A note on the yaw attitude modeling of BeiDou IGSO-6, a report dated November 20, 2017. http://navigation-office.esa.int/attachments_24576369_1_BeiDou_IGSO-6_Yaw_Modeling.pdf. Accessed 21 Jan 2018
- Dilssner F, Springer T, Enderle W (2011a) GPS IIF yaw attitude control during eclipse season. AGU Fall Meeting, San Francisco. http://acc.igs.org/orbits/yaw-IIF_ESOC_agu11.pdf. Accessed 9 Dec 2011
- Dilssner F, Springer T, Gienger G, Dow J (2011b) The GLONASS-M satellite yaw-attitude model. *Adv Space Res* 47(1):160–171. <https://doi.org/10.1016/j.asr.2010.09.007>
- Dilssner F, Laufer G, Springer T, Schonemann E, Enderle W (2018) The BeiDou attitude model for continuous yawing MEO and IGSO spacecraft. EGU 2018, Vienna. http://navigation-office.esa.int/attachments_29393052_1_EGU2018_Dilssner_Final.pdf. Accessed 21 Jan 2018
- Ebert K, Oesterlin W (2005) Dynamic yaw steering method for space-craft. European patent specification EP 1526072B1. <http://www.freepatentsonline.com/EP1526072.pdf>. Accessed 21 Jan 2018
- GSA (2017) Galileo satellite metadata. <https://www.gsc-europa.eu/support-to-developers/galileo-satellite-metadata>. Accessed 28 Nov 2017
- Guo J, Zhao Q, Geng T, Su X, Liu J (2013) Precise orbit determination for COMPASS IGSO satellites during yaw maneuvers. In: Sun J, Jiao W, Wu H, Shi C (eds) Proc. China satellite navigation conference (CSNC) 2013, vol III. 245:41–53. https://doi.org/10.1007/978-3-642-37407-4_4
- Guo J, Xu X, Zhao Q, Liu J (2016) Precise orbit determination for quad-constellation satellites at Wuhan University: strategy, result validation, and comparison. *J Geodesy* 90(2):143–159. <https://doi.org/10.1007/s00190-015-0862-9>
- Guo J, Chen G, Zhao Q, Liu J, Liu X (2017) Comparison of solar radiation pressure models for BDS IGSO and MEO satellites with emphasis on improving orbit quality. *GPS Solut* 21(2):511–522. <https://doi.org/10.1007/s10291-016-0540-2>
- Ishijima Y, Inaba N, Matsumoto A, Terada K, Yonechi H, Ebisutani H, Ukawa S, Okamoto T (2009) Design and development of the first quasi-zenith satellite attitude and orbit control system. In: Proceedings of the IEEE aerospace conference, Big Sky, 7–14 March. <https://doi.org/10.1109/AERO.2009.4839537>
- Kouba J (2009) A simplified yaw attitude model for eclipsing GPS satellites. *GPS Solut* 13(1):1–12. <https://doi.org/10.1007/s10291-008-0092-1>
- Kouba J (2017) Notes on December 2017 version of the ECLIPS subroutine. http://acc.igs.org/orbits/eclips_Dec_2017.tar. Accessed 21 Jan 2018
- Kuang D, Desai S, Sibois A (2017) Observed features of GPS block IIF satellite yaw maneuvers and corresponding modeling. *GPS Solut* 21(2):739–745. <https://doi.org/10.1007/s10291-016-0562-9>
- Liu J, Ge M (2003) PANDA software and its preliminary result of positioning and orbit determination. *Wuhan Univ J Nat Sci* 8:603–609. <https://doi.org/10.1007/BF02899825>
- Liu Y, Jia X, Ruan R (2017) BeiDou IGSO satellite orbit precision analysis based on new attitude control mode. *J Geodesy Geodyn* 37(6):614–617. <https://doi.org/10.14075/j.jgg.2017.06.012>

Montenbruck O, Schmid R, Mercier F, Steigenberger P, Noll C, Fatkulin R, Kogure S, Ganeshan AS (2015) GNSS satellite geometry and attitude models. *Adv Space Res* 56(6):1015–1029. <https://doi.org/10.1016/j.asr.2015.06.019>

Montenbruck O et al (2017a) The multi-GNSS experiment (MGEX) of the International GNSS Service (IGS)—achievements, prospects and challenges. *Adv Space Res* 56(7):1671–1697. <https://doi.org/10.1016/j.asr.2017.01.011>

Montenbruck O, Steigenberger P, Darugna F (2017b) Semi-analytical solar radiation pressure modeling for QZS-1 orbit-normal and yaw-steering attitude. *Adv Space Res* 59(8):2088–2100. <https://doi.org/10.1016/j.asr.2017.01.036>

Steigenberger P, Hauschild A, Montenbruck O, Rodriguez-Solano C, Hugentobler U (2013) Orbit and clock determination of QZS-1 based on the CONGO network. *Navigation* 60(1):31–40. <https://doi.org/10.1002/navi.27>

Wu JT, Wu SC, Hajj GA, Bertiger WI, Lichten SM (1993) Effects of antenna orientation on GPS carrier phase. *Manuscr Geod* 18:91–98

Zhao Q, Chen G, Guo J, Liu J, Liu X (2017) An a prior solar radiation pressure model for the QZSS Michibiki satellite. *J Geodesy*. <https://doi.org/10.1007/s00190-017-1048-4>

Zhao Q, Wang C, Guo J, Wang B, Liu J (2018) Precise orbit and clock determination for BeiDou-3 experimental satellites with yaw attitude analysis. *GPS Solut* 22:4. <https://doi.org/10.1007/s10291-017-0673-y>



Qile Zhao is a professor at GNSS Research Center of Wuhan University. He received his Ph.D. degree from Wuhan University in 2004. In 2006–2007, as a post-doctoral fellow, he did his post-doctoral program in DEOS, Delft University of Technology, The Netherlands. His current research interests are precise orbit determination of GNSS and low earth orbiting satellites, and high-precision positioning using GPS, Galileo and BDS systems.



Jingnan Liu graduated from the former Wuhan College of Surveying and Mapping in 1967 and received his master's degree in 1982. He was elected Academician of the Chinese Academy of Engineering in 1999. Since 1998, he has been in charge of the National Engineering Research Center for Satellite Positioning System. He has been a member of the Science and Technology Committee, Ministry of Education of China in 1997–2009 and as an editorial board member of GPS Solutions

in 1998–2000. He is currently an executive member of the council, Chinese Society for Geodesy, Photogrammetry and Cartography; the editorial board member of GPS World; and the coordinator of IGS.



Chen Wang is a Ph.D. student at GNSS Research Center, Wuhan University, currently. He received his bachelor degree at College of Geology Engineering and Geomatics, Chang'an University, in 2014. His research focuses on GNSS data processing and precise orbit determination.



Jing Guo is a postdoctoral researcher at GNSS Research Center of Wuhan University. He received his bachelor, master and doctor degrees at Wuhan University in 2009, 2011 and 2014, respectively. Currently, he works on GNSS data processing, particularly the precise orbit determination for multi-GNSS satellites, and is also responsible for the routine data processing of MGEX and iGMAS at Wuhan University.